

## Direct measurement of aerodynamic pressure above a simple progressive gravity wave

By OMAR H. SHEMDIN† AND EN YUN HSU

Department of Civil Engineering, Stanford University, Stanford, California

(Received 16 January 1967 and in revised form 13 June 1967)

Measurements of the aerodynamic pressure distribution at the interface between air and simple progressive water waves are obtained with the use of a pressure sensor that follows the water surface. The theory of Miles (1957, 1959) and Benjamin (1959) on shear flows past a wavy boundary predicts a phase shift between the pressure distribution along the boundary and the boundary itself. An experimental verification of this theory is sought especially. A wind-wave facility 115 ft. long, 6 ft. high and 3 ft. wide was used. The facility is equipped with an oscillating-plate wave-generator which is capable of generating sinusoidal or arbitrary wave-forms, and a suction fan which can produce wind velocities up to 80 ft./sec when the water is at a nominal depth of 3 ft. The pressure sensor used for the measurements of pressure, was mounted on an oscillating device such that the sensor could be maintained at a fixed small distance (within  $\frac{1}{4}$  in.) above a propagating wavy surface at all times. The perturbation pressure over progressive waves is extracted from recorded data sensed by the moving sensor. The results compare favourably with the theoretical predictions of Miles (1959).

---

### 1. Introduction

Since the comprehensive review of wind-generated waves presented by Ursell (1956), significant theoretical and experimental progress in wind-wave research has been made. Two theories for the generation of water waves have been proposed. The first, proposed by Phillips (1957), is based on resonance between the water surface and the random pressure fluctuations inherent in a turbulent velocity field. The second, proposed by Miles (1957, 1959) and Benjamin (1959), is based on interaction between the air shear velocity profile and the perturbed water surface. More recently, Hasselmann (1966) described a wave-wave interaction theory which incorporates both the resonance and the shear interaction mechanisms as special cases.

A number of experimental attempts have been made to establish the validity of the advanced theories, both under laboratory conditions, such as the studies made by Cox (1958), Cohen & Hanratty (1965), Hidy & Plate (1966), and Wiegell & Cross (1966), and in the ocean, such as the studies made by Longuet-Higgins (1962), and Snyder & Cox (1966). It is recognized that the actual experiments of

† Now at Department of Coastal and Oceanographic Engineering, University of Florida, Gainesville, Florida.

Longuet-Higgins were conducted before the advancement of the new theories; however, the results were used at a later date to infer the validity of the newly advanced theories. The results obtained by the above authors have been instrumental in obtaining a qualitative description of the growth of waves, and inferences were made as to the validity of the above theories from the measured rates of growth and/or the measurements of pressures in the air. The results, however, leave much to be desired in the way of conclusive verification of the theoretically suggested growth mechanisms and the regimes of flow under which they become efficient in transferring energy from air to water.

According to Miles's theory, the shear interaction between an air boundary layer  $U(y)$  and a simple (monochromatic) water wave, propagating with phase speed  $c$ , emphasizes the role of a critical layer at a height  $y_c$  above the water surface, at which energy transfer takes place between air and water. The critical-layer height is defined by  $U(y_c) = c$  and is considered to be larger than the laminar sublayer. The viscous effects are assumed to play an insignificant role in energy transfer. Under such conditions, the inviscid Reynolds stress plays a dominant role in energy transfer from air to water. Below the critical layer, in  $y < y_c$ , the inviscid Reynolds stress brings about a phase shift in the normal aerodynamic pressure distribution such that a higher pressure is exerted on the upstream slope of the wave compared with the downstream slope.

The aim of the present investigation is to provide direct experimental verification of the inviscid Reynolds-stress mechanism responsible for the transfer of energy from air to water. The air pressure distribution at the critical layer above a progressive wave is measured. An oscillating device (or wave follower) was designed on which a pressure sensor was mounted and maintained at a small fixed distance above the water surface at all times.

The importance of measuring the pressure below the critical layer was demonstrated by the authors (Shemdin & Hsu 1966) by comparing pressure records obtained from a pressure sensor fixed in space above the mean water level, to records obtained from the same sensor following the water surface. The perturbation pressure obtained by a moving pressure sensor was in accord with the theoretical predictions while the perturbation pressure obtained by a fixed pressure sensor was only in accord with the theoretical predictions when the fixed pressure sensor remained in the critical layer.

## 2. Theoretical considerations

### 2.1. Review of the inviscid Reynolds-stress mechanism

The mathematical model of Miles (1957) is defined by the following assumptions: the air flow is assumed to be inviscid and incompressible, and, in the absence of waves, to be parallel and to have a mean velocity profile  $U(y)$ . The surface waves have the form (the real part is taken to describe the actual wave-form)

$$\eta = a \exp\{ik(x - ct)\}, \quad (2.1)$$

where  $k$  is the wave-number and  $ka \ll 1$ . The waves propagate at the air-water interface with a speed  $c$ . The disturbances in the air flow induced by the surface

waves are assumed to be small, so that the equations of motion can be linearized. In addition, the perturbations in the turbulent fluctuations are neglected in the model.

The aerodynamic pressure on the surface of progressive waves  $P_{as}$  was assumed to have the form

$$P_{as} = (\alpha + i\beta)\rho_a U_1^2 k\eta, \quad (2.2)$$

where  $\alpha$  and  $\beta$  are real constants,  $\rho_a$  is the air density, and

$$U_1 = 2.5U_*.$$

The constant  $\alpha$  and  $\beta$  were determined by solving the inviscid Orr–Sommerfeld equation for an assumed logarithmic velocity distribution specified by

$$U(y) = U_1 \ln \frac{y}{z_0}, \quad (2.3)$$

where  $z_0$  is the roughness height.

The effect of the pressure on the surface waves can be evaluated by solving the boundary-value problem for the wave motion in water. The water motion is assumed to be inviscid, incompressible, and irrotational. It can be shown that the propagation speed of the surface wave  $c$  can be expressed

$$c \approx c_0 \left[ 1 + \frac{1}{2}(\alpha + i\beta) \frac{\rho_a}{\rho_w} \left( \frac{U_1}{c_0} \right)^2 \right], \quad (2.4)$$

where

$$c_0 = \sqrt{g/k}.$$

Substituting (2.4) in (2.1) yields

$$\eta = a \exp \left\{ \frac{\beta \rho_a}{2 \rho_w} \left( \frac{U_1}{c_0} \right)^2 k c_0 t \right\} \exp \{ ik(x - c_0 t) \}, \quad (2.5)$$

where the assumption

$$\frac{\alpha \rho_a}{2 \rho_w} \left( \frac{U_1}{c_0} \right)^2 \ll 1$$

was made. It can be seen from (2.5) that the rate of growth of the waves caused by shear flow is exponential. It is also seen that the magnitude of the aerodynamic surface pressure can be calculated from (2.2) for known values of  $\alpha$  and  $\beta$ . The phase shift  $\theta$  between the surface pressure distribution and the wave is given by

$$\theta = \tan^{-1} \frac{\beta}{\alpha}. \quad (2.6)$$

## 2.2. Pressure measurement from an oscillating frame of reference

The motion of the pressure sensor produces external flow disturbances around the sensor as well as internal flow disturbances in the tubing that connects the sensor to the pressure transducer. In order to minimize the external flow disturbances, a thin, circular, dish-shaped sensor with a piezometer hole at its geometric centre is used. If the external flow disturbances can be neglected, the relationship between the pressure fields in a moving frame of reference and in a fixed frame of reference can be evaluated by a simple co-ordinate transformation (Lamb 1945, section 12). The internal flow disturbance caused by the motion of the tubing wall

through viscous action is determined experimentally. Meaningful comparisons between the experimental results and the theoretical predictions of Miles and Benjamin can only be made if the effects caused by the external and internal flow disturbances are properly evaluated.

The relationships between the two frames of reference are

$$x = X; \quad y = Y + a \exp(ikcT); \quad t = T, \quad (2.7)$$

where  $(x, y, t)$  and  $(X, Y, T)$  are the space and time co-ordinates in both the fixed and the moving frames respectively. A function  $f(x, y, t)$  expressed in the fixed frame of reference can be described in terms of the moving co-ordinates by (2.7)

$$f(x, y, t) = f[x(X, Y, T), y(X, Y, T), t(X, Y, T)]. \quad (2.8)$$

It follows that

$$\frac{\partial f}{\partial x} = \frac{\partial f}{\partial X}; \quad \frac{\partial f}{\partial y} = \frac{\partial f}{\partial Y}; \quad \frac{\partial f}{\partial t} = \frac{\partial f}{\partial T} - ikac \exp(ikcT) \frac{\partial f}{\partial Y}. \quad (2.9)$$

Using the relationships (2.9), it can be shown that the inviscid Orr–Sommerfeld equation remains invariant when the perturbed flow field is described in the moving frame of reference. Furthermore, it can be shown that the boundary conditions for a flow described in the oscillating frame of reference are identical to those prescribed in the fixed frame of reference, so long as the wave slope is small ( $ka \ll 1$ ). It can be concluded that the solutions of the boundary-value problem obtained by both Miles and Benjamin are equally valid for the flow field in the oscillating frame of reference. Direct comparison between the experimental results and the theoretical predictions can be made provided appropriate corrections for internal flow disturbances are made.

The spurious pressure signals caused by motion of the pressure sensing system is determined experimentally. Since the shape of the pressure sensor was selected to produce negligible external flow disturbances, the internal flow disturbance is independent of wind speeds and depends only on the amplitude and frequency of oscillation of the system. The pressure signal caused by the motion of the sensor was evaluated systematically under zero wind speed for the following test conditions: (i) sensor oscillates sinusoidally above an undisturbed free surface, (ii) sensor oscillates and follows a sinusoidal progressive wave, (iii) sensor fixed in space above a sinusoidal progressive wave. Upon comparison of the pressure signals thus obtained, it was concluded that the viscous induced motion in the tubing produced a pressure signal in phase with the sinusoidal motion of the sensor in the range of frequencies investigated. The amplitude of the viscous induced motion was also deduced from the above comparison.

### 2.3. Boundary-layer control

Preliminary measurements of wind velocity profile in the wind-wave facility indicated an extremely thin critical layer. For example, the critical layer was found to be of the order of 0.01 in. for a maximum wind speed of 20 ft./sec and a wave frequency of 1 c/s. Because of the finite size of the pressure sensor, it becomes practically impossible to embed the sensor near the interface below

the critical layer even when the sensor follows the wavy surface. Thickening of the boundary layer is necessary. From (2.3) it is seen that

$$y_c = z_0 \exp(c/U_1). \quad (2.10)$$

Thus, the height of the critical layer can be increased by increasing the roughness height  $z_0$ . For this purpose, a 5 ft. long transition plate with 1 in. height roughness elements was installed at the air inlet to the test section. The critical-layer height was found to increase to 1 in. for the maximum wind speed of 20 ft./sec and 1 c/s wave, and to be satisfactory for subsequent experiments.

### 3. Experimental apparatus

#### 3.1. *The wind-wave facility and instrumentation*

The newly constructed wind-wave facility in the Hydraulics Laboratory at Stanford University was used for the study. A detailed description of this facility was given by Hsu (1965). The channel is 115 ft. long, 6 ft. high and 3 ft. wide. The test section is 85 ft. long and is constructed with glass walls for visual observation of waves. The entire channel is enclosed with a set of 5 ft. long steel roof-plates at the top of the channel. A separate 5 ft. long aluminium plate, used for mounting the wave follower and other instruments, was designed to replace conveniently any one of the regular steel-roof cover plates. Consequently measurements could be made at any distance along the test section.

The wave generator is a horizontal, displacement-type oscillating plate. It is driven by a hydraulic power cylinder and controlled by an electro-hydraulic power system, so that the motion of the plate may respond to an arbitrary input electrical signal. Sinusoidal waves, ranging in frequency from 0.2 to 4.0 c/s, can be generated. Solitary waves and waves of complex shape can also be generated by the system. To absorb the energy of the generated waves, a beach is installed at the downstream end of the channel. The reflexion coefficients of the beach for waves ranging in frequency from 0.6 to 1.2 c/s was found to be less than 10%.

The air intake is located 17 ft. downstream of the mean position of the wave generator plate so that the generated waves become fully established (a minimum horizontal distance three times the water depth is required) before exposure to the action of wind. The air intake is elbow-shaped and is augmented with three turning vanes inside the elbow, a wire screen, and a 2 in. wide honeycomb with  $\frac{1}{4}$  in. hexagonal matrix at the inlet to the test section. These ensure the proper shape of the boundary-layer profile and minimize the angularity of the incoming flow. The elevation of the air intake can be adjusted with respect to the channel frame up to approximately 12 in. It is normally set at about 6 in. above the free surface for a nominal water depth of 3 ft. A suction fan is provided at the downstream end of the channel. The fan is driven by a motor capable of creating a maximum free-stream air velocity of 80 ft./sec with a nominal water depth of 3 ft. The speed of the fan can be controlled to  $\pm 1$  rev/min at all speeds.

To thicken the boundary layer, a roughened transition plate was installed in the wind-wave facility, as is shown in figure 1. The 5 ft. long, 3 ft. wide transition plate was artificially roughened by roughness elements 1 in. in height. The roughness elements were made from  $\frac{1}{2}$  in. diameter dowels and were glued to the sur-

face of the plate at a spacing of 1 in. on centres, and staggered between rows. A downward slope of 1 to 17 of the transition plate was provided to ensure a smooth transition between the wind stream and the wave train.

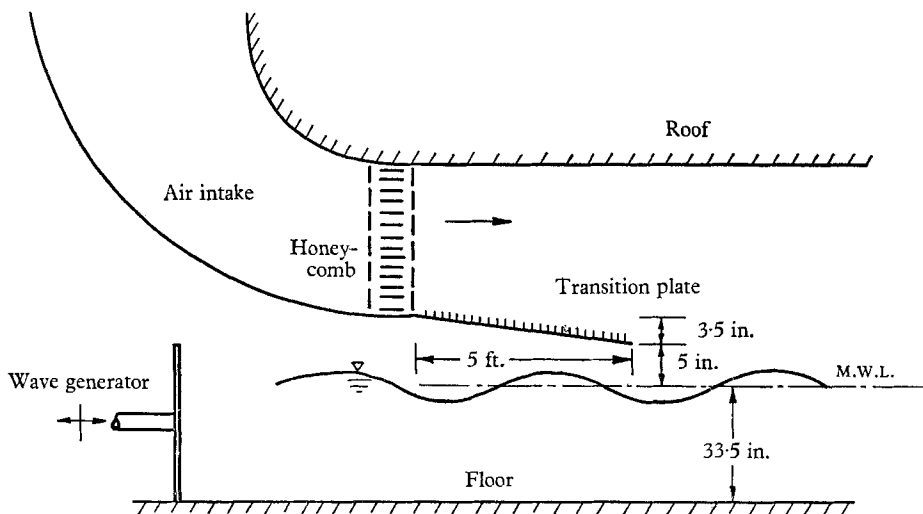


FIGURE 1. Air intake and rough transition plate.

The air velocity was measured by using a Pitot-static probe in conjunction with a sensitive pressure transducer and a Sanborn 650 optical-type recorder. The  $\frac{1}{32}$  in. o.d. Pitot-static probe used is a standard shelf item manufactured by United Sensors and Control Corporation. The pressure transducer used had a full range of  $\pm 1$  in. of water ( $\pm 0.037$  psi) and was manufactured by Pace Instrument Company (model P 90 D). A static calibration of the transducer and the recording system was obtained with the use of a Harrison micromanometer. Mean velocities at each elevation above the mean water level were obtained and both temperature and humidity effects were taken into account when converting dynamic pressure data into velocities.

Wave-height measurements were obtained by a capacitance type wave-height gauge and a capacitance bridge along with a Sanborn 650-1100 series optical-type recorder. A more detailed description of the wave-height measuring system is given in Shemdin & Hsu (1966).

### 3.2. *The wave-following, pressure-sensing system*

The wave-following, pressure-sensing system can be briefly described in three distinct subsystems: (a) a mechanical subsystem capable of holding a pressure sensor that can move freely in the vertical direction; (b) an electronic subsystem to control the vertical motion of the sensor such that the sensor can be maintained at a fixed small distance above a changing water surface elevation, and (c) a pressure-sensing subsystem to measure and record instantaneous pressures.

The mechanical subsystem is made of a cylinder on which the pressure sensor is mounted. The cylinder can oscillate freely inside another cylinder that is fixed in space with respect to the wind-wave facility. The position of the moving

cylinder is controlled by an electric motor. The mechanical subsystem is shown in figure 2, plate 1. The position of the pressure sensor is controlled by the local wave-height elevation through the use of a wave-height gauge (elevation control gauge) which is shown in figure 2, plate 1. The error of the pre-selected pressure sensor position about a mean level just above the water surface, is detected by a position indicator gauge which is also shown in figure 2, plate 1. In addition, a fixed wave-height gauge is provided with the pressure sensing system, as shown in figure 2, plate 1, since the prime objective of the study requires the simultaneous measurement of aerodynamic pressure near the water surface and the water-surface elevation.

The pressure-sensing subsystem is made of (1) a disk-shaped pressure sensor which is held close to the water surface and is connected to one side of (2) the Pace differential pressure transducer. The transducer is mounted on to the oscillating cylinder. The other side of the pressure transducer is connected to (3) a reference static pressure sensor which is identical to the first, but is kept at a large distance above the water surface in the unperturbed air stream. The entire pressure-sensing subsystem moves as a unit when following the water surface. Consequently the strenuous pressures caused by the deformation of the tubings are eliminated. The present scheme was devised after less successful trials in which the transducer was kept fixed in space relative to the moving pressure sensor. The motion of the transducer produces negligible effects on the pressure measurements, since the Pace transducer is based on the variable-reluctance principle. According to the specifications furnished by the manufacturer, the acceleration sensitivity of the transducer is 0.001 psi/g in the more sensitive direction (normal to the diaphragm). The orientation of the transducer diaphragm in this investigation was parallel to the direction of motion so that the motion of the transducer produced no significant effect on the pressure measurements.

The entire sensing system was calibrated for frequency response. The pressure sensor was placed inside a pressure chamber, in which the pressure could be varied sinusoidally at a fixed small amplitude and for frequencies ranging from 0.3 to 3.5 c/s. During calibration the reference static sensor was left outside the pressure chamber. The system was calibrated with and without the superposition of external electrical damping. The damping is necessary to eliminate higher-frequency pressure fluctuation due to electrical or mechanical effects.

#### **4. Experimental procedure**

The verification of the proposed mechanisms of energy transfer from air to water requires the investigation of (a) the air velocity profile above a perturbed water surface, and (b) the measurement of air pressure as close as possible to the interface between air and water. In the present investigation the measurements of air velocity and aerodynamic pressure at the interface between air and water were obtained in separate runs. The reproducibility of experimental conditions in the wind-wave facility is within 1%, however. Mean velocity profiles were obtained above mechanically generated waves having specified frequencies and amplitudes. The procedure followed was to record the mean dynamic head of the

Pitot-static probe at each vertical position above the mean water level, and to plot the velocities with respect to the mean water level. In the present investigation, all the velocity profiles were taken at station 17.5 or 17.5 ft. downstream from the air intake. The range of the free-stream velocities measured was from zero to 40 ft./sec.

The aerodynamic pressure at the interface between air and water was measured under the same experimental condition for which air velocity profiles were obtained. The procedure followed was to generate the desired mechanical wave and to allow the pressure sensor to follow the water surface at a distance of approximately  $\frac{1}{2}$  in. above the water surface. Then the wind speed was increased in small increments from zero to 40 ft./sec. At each wind speed the pressure data consisted of simultaneous recordings of the wave profile, the surface pressure, and the position error of the pressure sensor about a pre-selected mean position above the instantaneous water surface.

Undesirable high-frequency pressure fluctuations (compared with wave frequency) caused by electrical noise, aerodynamic turbulent fluctuations, and mechanical vibrations of the apparatus were eliminated by externally superposing capacitance on the signal obtained from the pressure transducer. Pressure fluctuations, having frequencies one order of magnitude larger than the wave frequency, could be eliminated without affecting the perturbation pressure resulting from the perturbed water surface. However, the addition of sufficient capacitance, to filter out some undesirable lower-frequency pressure fluctuations inherent in the oscillating system, caused an amplitude reduction and a phase lag in the pressure signal. The effect of the externally added capacitance on the transducer signal was accounted for in the present investigation.

A sample of the direct recordings of pressure is given by Shemdin & Hsu (1966). A typical record indicates a periodic variation of the perturbation pressure with a frequency equal to that of the mechanically generated wave. The record also shows additional random high-frequency fluctuations superimposed on the periodic variation which are attributed to the motion of the pressure-sensing system and the inherent electronic noise. In order to obtain more meaningful results from the data, an averaging procedure was used which is equivalent to folding a long pressure record over itself three or four times in such a way as to preserve the phase relationship between the pressure perturbation and the surface wave. A least-square sinusoidal fit to the superimposed records was calculated to yield the amplitude and phase angle of the best fit sine curve.

## 5. Experimental results

The mean velocity profiles for an air stream over a 0.4 c/s mechanically generated waves having a wave height of 4.15 in. is shown in figure 3, for blower settings between 40 to 200 rev/min. A logarithmic distribution is fitted to the velocity data for each blower setting, by the method of least squares. Although, at first sight, a logarithmic approximation seems reasonable, the data exhibit a systematic deviation from the least-square logarithmic fit. For the purpose of the present study, the logarithmic distribution facilitates the use of Miles's theory in predicting the amplitude and the phase angle of the perturbation pressure above the

water wave. The latter calculations are shown in table 1. Similar behaviour was observed for velocity profiles above waves of different frequencies.

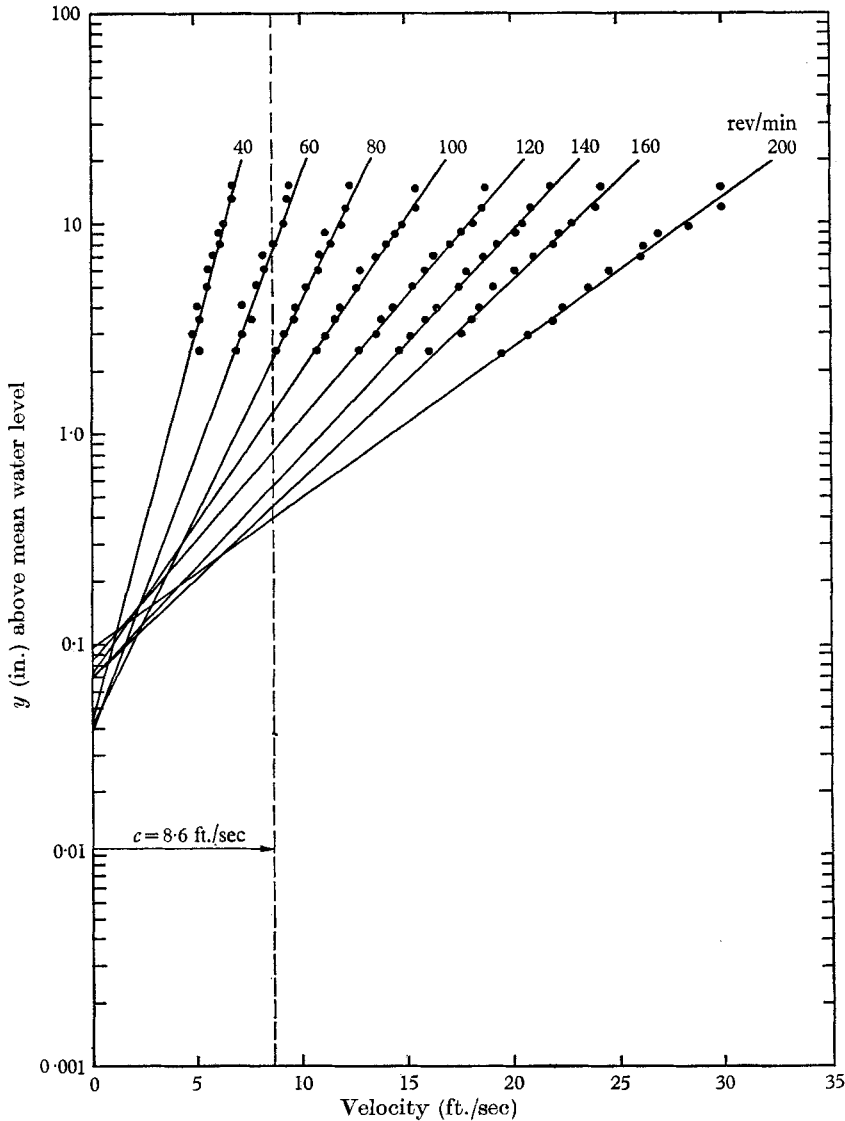


FIGURE 3. Mean velocity profiles for mechanically generated wave propagating with phase speed 8.60 ft./sec. Wave height = 4.15 in., wave frequency = 0.4 c/s.

The critical-layer heights are obtained from the velocity profiles shown in figure 3. The changes in the critical-layer height with increasing wind speed are shown in figure 4. The locations of the pressure sensor near the interface and the reference static sensor in the free stream are also shown in figure 4. It is seen that the reference static sensor will remain above the critical layer for maximum wind speeds greater than 7.5 ft./sec, and the pressure sensor near the interface will remain below the critical layer for maximum wind speeds less than 22 ft./sec.

Therefore, the meaningful velocity range to verify the inviscid Reynolds-stress mechanism is  $7.5 < V_{\max} < 22$  ft./sec.

Blower (rev/min)	40	60	80	100	120	140	160	200
$V_{\max}$ (ft./s)	6.5	9.5	12.00	15.5	18.5	21.5	24.0	30.0
$U_{\text{ave}}$ (ft./s)	5.7	8.2	10.5	13.0	15.6	18.2	20.4	23.6
$U_1$ (ft./s)	1.16	1.61	2.14	2.99	3.73	4.07	4.57	6.06
$U_*$ (ft./s)	0.46	0.64	0.85	1.2	1.49	1.63	1.82	2.43
$z_0$ (in.)	0.043	0.037	0.042	0.073	0.084	0.069	0.069	0.098
$\Omega$	0.8450	0.0388	0.0243	0.0219	0.0162	0.0113	0.0890	0.0071
$y_c$ (in.)	74.00	7.60	2.30	1.30	0.84	0.56	0.45	0.40
$c/U_1$	7.41	5.44	4.01	2.87	2.30	2.11	1.88	1.42
$\xi_c = ky_c$	1.78	0.1830	0.0550	0.0314	0.0203	0.0135	0.0108	0.0096
$\beta$	—	1.5	2.8	3.0	3.2	3.3	3.4	3.1
$-\alpha$	—	0.6	2.8	4.6	6.3	8.2	9.4	9.6
$\theta$ (deg.)	—	104	135	147	153	158	160	162
$ p_{\text{asl}} $ (psi)	—	$3.34 \times 10^{-6}$	$0.15 \times 10^{-4}$	$0.40 \times 10^{-4}$	$0.79 \times 10^{-4}$	$1.17 \times 10^{-4}$	$1.67 \times 10^{-4}$	$2.96 \times 10^{-4}$
$\left(\frac{ p_{\text{asl}} }{\rho_a g a}\right)$	—	$3.76 \times 10^{-2}$	0.17	0.45	0.89	1.31	1.88	3.32

TABLE 1. Data and theoretical calculations of pressure for mechanically generated wave propagating with phase speed 8.60 ft./sec. Wave height = 4.15 in., wave frequency = 0.4 c/s

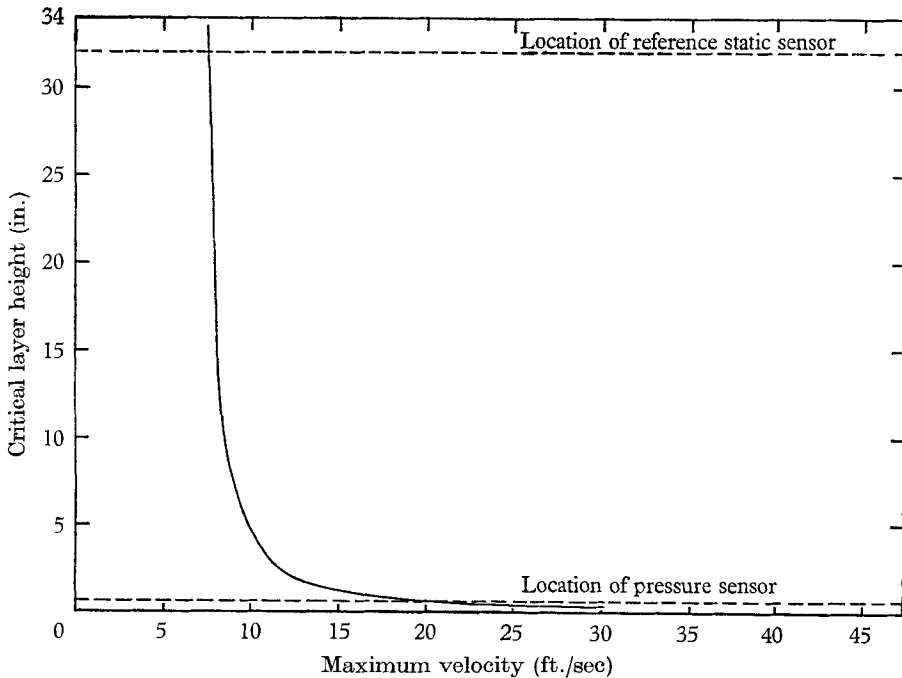
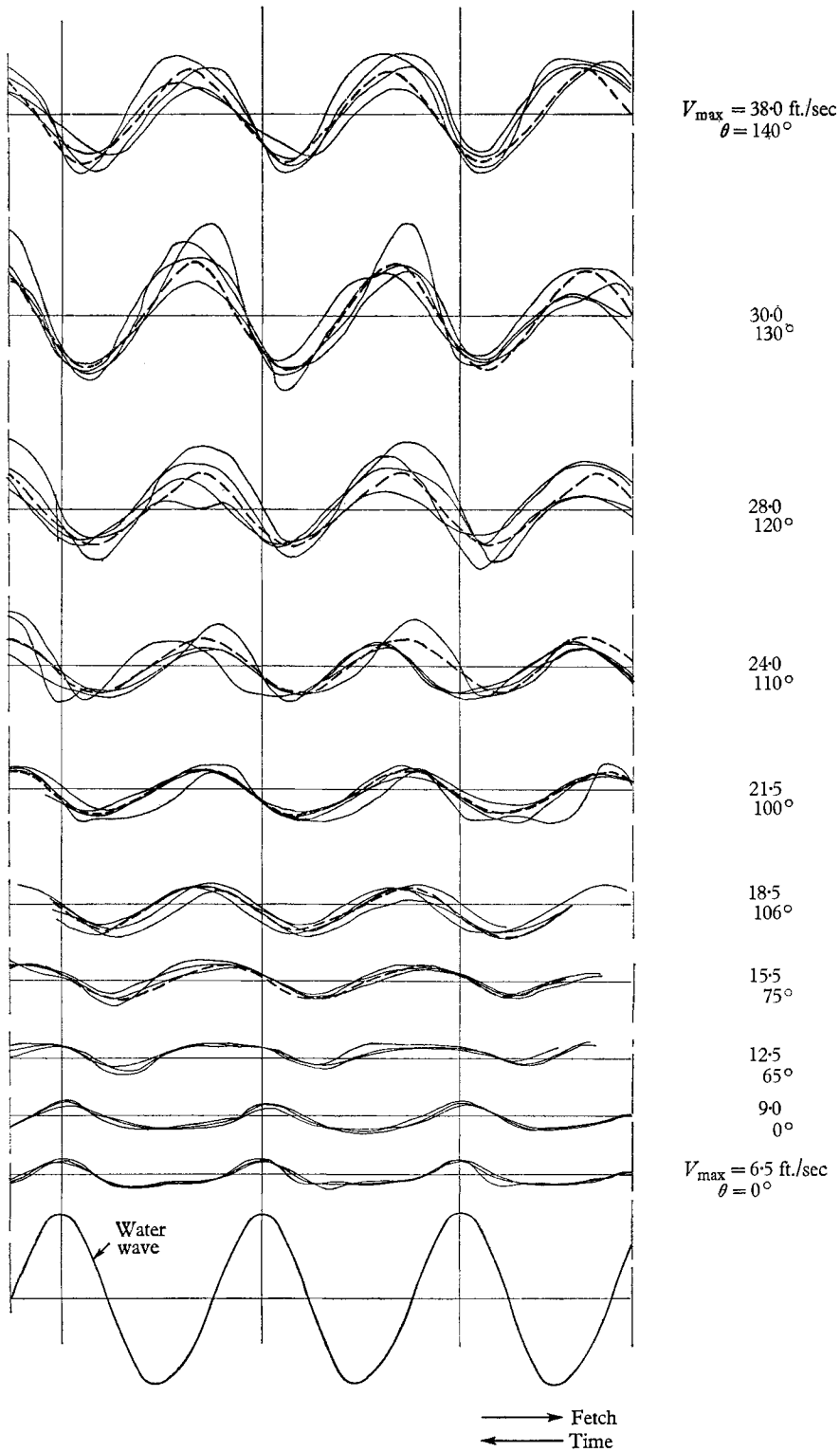


FIGURE 4. Critical height versus maximum wind speed for mechanically generated wave propagating with phase speed 8.60 ft./sec.

The sequence of superimposed pressure signals with increasing wind speed, obtained by allowing the pressure sensing system to follow the water surface, is shown in figure 5. A definite phase shift is observed with increasing wind speeds. It is to be noted that the pressure data shown in figure 5 include the dynamic



**FIGURE 5.** Pressure distributions at different wind speeds for mechanically generated wave propagating with phase speed 8.60 ft./sec. Wave frequency = 0.4 c/s, wave height = 5.00 in., pressure sensor following water surface. —, data; ---, best fit sine curve.

effects due to the motion of the pressure-sensing system. The dynamic effects, however, depend on the amplitude and frequency of oscillation of the pressure-sensing system, and are independent of the wind speed. Consequently, the pressure signals in figure 5 contain the same dynamic effect at all wind speeds. The pressure shift at different wind speeds is seen to be strictly due to the inviscid Reynolds-stress mechanism acting in the critical layer.

$c/U_1$	$V_{\max}$	$U_{\text{ave}}$	$p_{as}/\rho_a g a$ measured	$p_{as}/\rho_a g a$ calculated	$\theta$ (degrees) measured	$\theta$ (degrees) calculated
$\infty$	0	—	1.07	—	180	—
10.0	4.0	4.0	0.22	—	180	—
7.41	6.0	5.7	0.07	—	180	—
5.44	9.5	8.2	0.07	0.04	0	104
4.01	12.0	10.5	0.42	0.17	125	135
2.87	15.5	13.0	0.68	0.45	125	147
2.30	18.5	15.6	1.18	0.89	148	153
2.11	21.5	18.2	1.52	1.31	151	158
1.88	24.5	20.4	2.20	1.88	153	160
1.70	27.5	22.0	3.30	—	149	—
1.42	30.5	23.6	3.83	3.32	159	162
1.20	38.0	30.5	8.10	—	172	—

TABLE 2. Comparison between theory and experiment for wave propagating with phase speed 8.60 ft./sec

A comparison between the experimental observations and the theoretical prediction of Miles (1959) requires the extraction of the interface pressure from the recorded pressure signal. The recorded pressure signal is a composite signal which depends on the perturbation pressure at the air-water interface sensed by the pressure sensor (connected to the positive side of the pressure transducer), the pressure sensed by the reference static sensor at  $y_\infty$  (connected to the negative side of the transducer), and the viscous effect in the tubing which connects the pressure sensor and the reference static sensor to the pressure transducer. Since the reference static sensor remains above the critical layer for  $V_{\max} > 7.5$  ft./sec as shown in figure 4, the pressure measured by the reference static sensor is assumed to be identical to that given by the potential solution (Lamb 1945, section 232). The assumption is reasonable when the critical-layer height is small compared with the height of the reference static sensor. The equation for the recorded pressure signal becomes (the effect of a restricted upper boundary is included):

$$\frac{\text{Recorded pressure signal}}{\rho_a g a} = \frac{p_{as}}{\rho_a g a} + \left[ \frac{U_a}{c} - 1 \right]^2 \frac{\cosh k(y_\infty - h)}{\cosh kh} \cos kct + \frac{p_d}{\rho_a g a} \cos kct, \quad (5.1)$$

where  $p_d$  is the pressure amplitude due to the motion of the pressure sensing system,  $p_{as}$  is the perturbation pressure at the water surface and  $h$  is the height of the upper boundary. The second term on the right-hand side of (5.1) is the inviscid pressure term sensed by the reference static sensor. The average velocity  $U_{\text{ave}}$  was used for  $U_a$  in (5.1) and the justification as well as the consequence of

this assumption will be discussed later. It is to be observed that  $p_a = 0$  in the absence of effects due to viscosity and geometric differences in the tubing. In order to extract the perturbation pressure at the air-water interface from the pressure data,  $p_a$  was determined experimentally as discussed in §2.2.

The comparison between the experimental results and the theoretically predicted values, according to Miles (1959), is presented in table 2 for the 0.4 c/s mechanically generated wave. In view of the difficulty in measuring small pressures (of the order of  $10^{-4}$  psi) and their phase angles, the comparison between the experimental data and the theoretical results appears to be in satisfactory agreement.

## 6. Discussion of results and conclusions

The results presented in table 2 provide a good check on the theory of Miles (1959). Perhaps the most critical assumption is that of substituting the average velocity  $U_{ave}$  for  $U_a$  in (5.1) instead of the maximum velocity  $V_{max}$  or some other reference velocity. The magnitude of the experimental pressure amplitude could increase by as much as 50% if  $V_{max}$  is used instead of  $U_{ave}$ . A justification for using  $U_{ave}$  is seen from the representation of the pressure component in phase with the wave trough given by (Benjamin 1959, section 7)

$$aR_e(P_s) = -k^2 a \int_0^\infty (U - c)^2 e^{-k\eta} d\eta. \quad (6.1)$$

The perturbation pressure in (6.1) reduces to the form given by the ideal fluid theory when  $U = U_a$ . The integration of  $U$  over the height above the water surface is seen as a form of averaging over the velocity profile.

The results presented in table 2 give strong support to the validity of the Miles-Benjamin theory under the conditions prescribed by the theory. The results also exhibit closer agreement for values of  $c/U < 4.0$ . The latter corresponds to a critical-layer height less than 3 in. and may be attributed to the assumption, made to determine the interface pressure, that the reference static sensor is in the region of irrotational motion.

The experimental approach followed in referencing the surface pressure to the free-stream pressure automatically cancels the effect of gravity on the wavy surface. Normally, the change in the air column above the water surface should be considered. Mathematically, it is taken into account by adding to the air perturbation pressure another component of pressure in phase with wave trough and having an amplitude equal to  $\rho_a ga$ . The effect of gravity on the measured perturbation pressure is one of increasing the amplitude and bringing the phase shift closer to in phase with the wave trough. The latter was demonstrated by Longuet-Higgins (1962).

The role of the tangential stress in transferring energy from air to water appears to be of secondary importance. Benjamin (1959) estimated that the tangential stress contributes a small percentage of the total energy transfer from air to water when compared with the normal stress, for waves progressing with a fair speed in the direction of flow. A direct experimental verification of the role of

energy transfer due to tangential stress is seen to be extremely difficult. It can be inferred from the agreement between the experimentally measured and theoretically predicted interface pressures, however, that the theoretical model proposed by Miles (1959) and Benjamin (1959) is a realistic one under the conditions in the theory. Therefore, under these conditions, it is inferred that the normal stress contributes most of the energy transfer from air to water.

In conclusion, it is seen that the results of this study provide a direct experimental verification of the theoretically proposed inviscid Reynolds stress mechanism in transferring energy from air to water under laboratory conditions. The results also indicate the importance of measuring the perturbation pressure below the critical layer.

This work was supported under a research program sponsored by the National Science Foundation under Grants GP-2401 and GK-736 and the Fluid Dynamic Branch of the Office of Naval Research, U.S. Navy, under Contract Nonr-225 (71), NR 060-320.

#### REFERENCES

- BENJAMIN, T. B. 1959 Shearing flow over a wavy boundary. *J. Fluid Mech.* **6**, 161.
- COHEN, L. S. & HANRATTY, T. S. 1965 Generation of waves in the co-current flow of air and a liquid. *A.I.Ch.E.* **11**, 138.
- COX, C. S. 1958 Measurement of slopes of high frequency wind waves. *J. Marine Res.* **16**, 199.
- HASSELMANN, K. F. 1966 Interactions between the ocean waves and the atmosphere. *6th Hydrodynamics Naval Symposium*, Washington, D.C.
- HIDY, G. & PLATE, E. 1966 Wind action on water standing in a laboratory channel. *J. Fluid Mech.* **26**, 651.
- HSU, E. Y. 1965 A wind-wave research facility. *Stanford University Department of Civil Engineering, Rept. 57*, Stanford.
- LAMB, H. 1945 *Hydrodynamics*. New York: Dover.
- LONGUET-HIGGINS, M. S. 1962 The directional spectrum of ocean waves and process of wave generation. *Proc. Roy. Soc. A* **265**, 286.
- MILES, J. W. 1957 On the generation of surface waves by shear flows. *J. Fluid Mech.* **3**, 185.
- MILES, J. W. 1959 On the generation of surface waves by shear flows. *J. Fluid Mech.* **6**, 568.
- PHILLIPS, O. M. 1957 On the generation of waves by turbulent wind. *J. Fluid Mech.* **2**, 417.
- SHEMDIN, O. H. & HSU, E. Y. 1966 Dynamics of wind in the vicinity of progressive waves. *Proc. 10th Conf. Coastal Eng., Tokyo*.
- SNYDER, R. L. & COX, C. S. 1966 A field study of the wind generation of ocean waves. *J. Marine Res.* **24**, 141.
- URSELL, F. 1956 Wave generation by wind. Article in *Surveys in Mechanics*. Cambridge University Press.
- WIEGEL, R. L. & CROSS, R. H. 1966 Generation of wind waves. *J. Waterways and Harbors Div., ASCE*, **92**, 1.

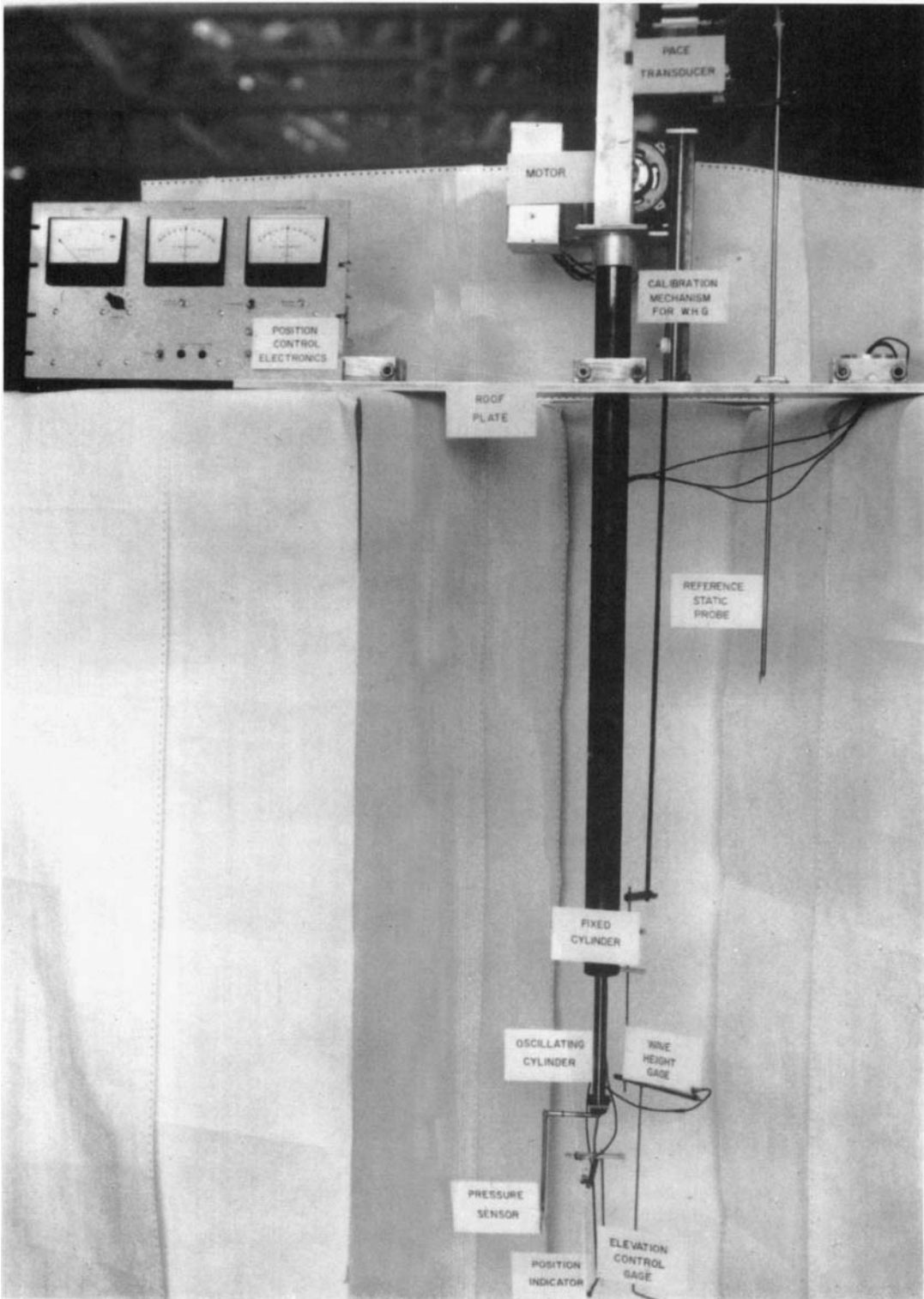


FIGURE 2. The wave-following, pressure-sensing system.

SHEMDIN AND HSU

(Facing p. 416)